Biophysical Chemistry, 37 (1990) 197–210
Elsevier

BIOCHE 01477

Precision determination and Adair scheme analysis of oxygen equilibrium curves of concentrated hemoglobin solution

A strict examination of Adair constant evaluation methods

Kiyohiro Imai

Department of Physicochemical Physiology, Medical School, Osaka University, Nakanoshima, Osaka 530, Japan

Received 29 January 1990
Accepted 26 February 1990

Hemoglobin; Adair constant; Oxygen equilibrium curve; Least-squares method

To examine the validity of the recent finding by Gill et al. (S.J. Gill, E. Di Cera, M.L. Doyle, G.A. Bishop and C.H. Robert, Biochemistry 26 (1987) 3995) that the third overall Adair constant (A_3) for human hemoglobin tetramers (Hb A) is too small to be determined and therefore that the contribution of the triply ligated species in the oxygenation process is negligibly small, highly accurate oxygen equilibrium curves for concentrated pure Hb A solutions were determined with an automatic oxygenation apparatus and analyzed by a least-squares curve-fitting method with various options. The present results indicate that an appropriate choice of weighting for data points is the key to the correct evaluation of the Adair constants and the present experimental data cannot accommodate the Adair scheme with $A_3 = 0$, giving distinctly positive values for A_3. Several criteria for correct determination of the Adair constants are presented.

1. Introduction

The oxygen equilibrium of tetrameric hemoglobin is described by the Adair equation [1],

$$Y = \frac{A_1 p + 2A_2 p^2 + 3A_3 p^3 + 4A_4 p^4}{4\left(1 + A_1 p + A_2 p^2 + A_3 p^3 + A_4 p^4\right)}, \qquad (1)$$

where Y denotes the fractional saturation of hemoglobin with oxygen, p the partial pressure of oxygen, and A_i ($i = 1$–4) the overall equilibrium constant for the binding of the first i oxygen molecules. This equation is of general validity as long as hemoglobin binds oxygen in a tetrameric form. The fractional population of the molecular species combining with i oxygen molecules at a given p is expressed by

$$f_i = \frac{A_i p^i}{1 + A_1 p + A_2 p^2 + A_3 p^3 + A_4 p^4} \quad (i = 0\text{–}4). \qquad (2)$$

If the α- and β-subunits of hemoglobin are entirely equivalent, both in their affinity for oxygen and in their manner of interaction, eq. 1 is rewritten as

$$Y = \left(K_1 p + 3K_1K_2 p^2 + 3K_1K_2K_3 p^3 + K_1K_2K_3K_4 p^4\right)\left(1 + 4K_1 p + 6K_1K_2 p^2 + 4K_1K_2K_3 p^3 + K_1K_2K_3K_4 p^4\right)^{-1}. \qquad (3)$$

Here, K_i ($i = 1$–4) which is related to the A terms as,

$$K_1 = A_1/4,\ K_2 = 2A_2/3A_1,\ K_3 = 3A_3/2A_2, \text{ and } K_4 = 4A_4/A_3, \qquad (4)$$

Correspondence address: K. Imai, Department of Physicochemical Physiology, Medical School, Osaka University, Nakanoshima, Osaka 530, Japan.

is the intrinsic (i.e., corrected for statistical factors) stepwise equilibrium constant corresponding to the i-th equilibrium,

$$Hb(O_2)_{i-1} + O_2 \rightleftarrows Hb(O_2)_i. \quad (5)$$

The cooperative nature of hemoglobin is well expressed by the Hill plot, i.e., $\log[Y/(1-Y)]$ vs $\log p$ [2]. Since

$$\log \frac{Y}{1-Y} = \log p + \log K_1 \text{ as } p \to 0 \quad (6)$$

and

$$\log \frac{Y}{1-Y} = \log p + \log K_4 \text{ as } p \to \infty, \quad (7)$$

the Hill plot possesses asymptotes with a slope of unity at the bottom and top ends and their intercepts on the ordinate at $\log p = 0$ give $\log K_1$ and $\log K_4$, respectively [3].

The four-step equilibrium constants (Adair constants) in eq. 1 or 3 were first determined by Roughton et al. [4–6] from accurate oxygen equilibrium curves which were measured by a gasometric technique. They paid particular attention to a precision determination of both ends of the curve (0–2% and 98–99.5% saturation) to an accuracy of 0.05% saturation as compared to that of 0.5% in the intermediate range (5–95%) and evaluated the Adair constants by fitting the Adair equation to the equilibrium curves by a least-squares method in which the end observed points were weighted 100-times more heavily than those of the intermediate range. They stressed that such a high-precision determination of the bottom and top ends of the curve was essential to the evaluation of the K terms with reasonable accuracy.

The author and his co-workers [3,7,8] determined accurate oxygen equilibrium curves for human adult hemoglobin (Hb A) under various conditions of solution and temperature with their automatic oxygenation apparatus [3,9,10] which combined a polarographic measurement of p with a spectrophotometric determination of Y. From those curves, they evaluated the Adair constants by a least-squares curve-fitting method in which the low- and high-range observed points were weighted according to a parabolic dependence of the standard error of Y on Y.

Recently, Gill and co-workers [11,12] attempted to determine the Adair constants from equilibrium curves measured by their thin-layer optical technique which combined the spectrophotometric measurement of Y with the stepwise, controlled change in p by means of a precision gas dilution valve. This technique is suitable for concentrated hemoglobin solutions while our apparatus is appropriate for dilute solution. They evaluated the Adair constants for concentrated Hb A solutions (2–12 mM on a heme basis) by a least-squares curve-fitting method with the observed points equally weighted, i.e., without weighting, and obtained an unanticipated result, namely, that the value of A_3 (β_3 according to their designation) was too low to be determined, indicating that the population of the triply ligated species was unmeasurably small [13]. When all the A terms were constrained to be nonnegative in the least-squares procedure, the best fit of A_3 was always zero, making the K_4 value undefinable. They further showed that the negligible contribution of the triply ligated species to the ligation process was also the case within the range of pH 6.95–9.10 [14], in the presence of different partial pressures of CO_2 [15], and even for carbon monoxide binding equilibrium [16].

As the likely cause of the obtaining of virtually zero values for A_3 by Gill et al., whereas we measured definitely positive values, Gill and coworkers [13] emphasized that the hemoglobin concentrations used by the latter group (60–600 μM) were so low that partial tetramer-to-dimer dissociation of hemoglobin could exert a significant influence on the observed Adair constants. Previously, Ackers and co-workers [17–19] stressed that the effect of dimeric species must be incorporated into the analysis of oxygen equilibrium data unless the hemoglobin concentration employed is greater than 1 mM.

Marden et al. [20] showed that the top part of the equilibrium curve from which the population and affinity of the triply liganded species are calculated is extremely sensitive to the normalization of the data, i.e., the conversion of absorbance values to oxygen saturation values. The normalization requires the determination of total absorbance change either by extrapolation or by

least-squares fitting. If A_3 is actually zero, then the following expression

$$\log\frac{Y}{1-Y} = 2\log p + \log\frac{A_4}{3A_2} \text{ as } p \to \infty \qquad (8)$$

holds instead of eq. 7 and the Hill plot shows an upper asymptote with a slope of 2. Therefore, strict experimental testing of the upper asymptote can be a key to the solution of the A_3 problem.

In the present study, highly accurate oxygen equilibrium curves for pure Hb A of high concentration (1.2 mM) were determined with our apparatus and analyzed in various manners in order to ascertain whether or not the experimental data can be accommodated within the Adair scheme with $A_3 = 0$. The current problems concerning the correct evaluation of the Adair constant will be extensively discussed from both experimental and analytical points of view and by comparing our technique with that of Gill and co-workers.

2. Materials and methods

2.1. Materials

Freshly prepared human whole hemolysate was passed through a Sephadex G-25 column equilibrated with 5 mM Tris and then deionized by passing through a Dintzis column [21]. Minor hemoglobin components were removed from the deionized hemoglobin solution as follows (H. Morimoto, unpublished data). Hb A_2 was removed on a CM-32 column which was equilibrated with sodium phosphate buffer (4.8 mM Na^+, 2.8 mM phosphate, pH 7.2). The Hb A_1 group was further removed on a DE32 column which was equilibrated with 5 mM Tris plus 1 mM acetate (pH 8.7). All these column procedures were carried out at 4°C in the presence of CO. No impurity was detected in the resultant hemoglobin sample as assessed by isoelectric focusing. Immediately before oxygen equilibrium measurements, the CO form was converted to the oxy form by illumination under a continuous stream of pure oxygen [22].

Phosphates were products of Merck. Bis-Tris, catalase, and superoxide dismutase were purchased from Sigma.

2.2. Methemoglobin content

Visible-range absorption spectra of hemoglobin were recorded on a double-beam spectrophotometer (model 320L, Hitachi). MetHb content was calculated from absorbance readings at 560, 576 and 630 nm by using the values of the millimolar absorption coefficient at different pH values [23].

2.3. Oxygen equilibrium measurements

Oxygen equilibrium curves were determined with an improved version [3,10] of our automatic oxygenation apparatus employed in the previous study [9]. The spectrophotometer used for the apparatus was a model Cary 118C (Varian Associates). The wavelength of the detection light was 620 nm and the path length of the oxygenation cell with movable windows [24] was set to 4.5 mm so that the total absorbance change upon deoxygenation of a 1.2 mM hemoglobin sample was approx. 0.6. Temperature within the cell was maintained constant within 25 ± 0.02°C. To minimize auto-oxidation of hemoglobin during measurement, catalase and superoxide dismutase were added to the sample to a concentration of 0.1 μM [25,26]. Although the slow response of the oxygen electrode was previously considered to be a major factor causing the disagreement between the deoxygenation and succeeding reoxygenation curves [9], metHb formation due to auto-oxidation has proved to be the more dominant factor. Therefore, the hemoglobin sample was deoxygenated and reoxygenated as quickly as possible without restricting the gas flow rate except for the air flow during the early stages of reoxygenation.

During the measurement, the absorbance and oxygen pressure data were acquired at real time by a personal computer (model PC-98XA; Nippon Electric, Tokyo), which was equipped with an Intel 80286 microprocessor and a 12-bit A/D converter. Absorbance data acquisition used one channel of the converter and the resolution was 0.00024 (= 1 absorbance unit/2^{12}). The dynamic

Table 1

Raw data of two deoxygenation curves measured under PHOS and BISTRIS conditions

PHOS			BISTRIS		
No.	p_{O_2}	Abs	No.	p_{O_2}	Abs
1	158.949	1.66412*E*-03	1	144.636	1.78080*E*-03
2	143.024	1.78080*E*-03	2	129.701	1.85857*E*-03
3	128.376	1.97523*E*-03	3	116.713	2.09189*E*-03
4	115.129	2.36411*E*-03	4	105.001	2.36411*E*-03
5	103.390	2.63633*E*-03	5	94.4892	2.48077*E*-03
6	92.7872	2.86967*E*-03	6	84.9049	2.63633*E*-03
7	83.2587	3.37520*E*-03	7	76.3321	2.90854*E*-03
8	74.7068	3.72519*E*-03	8	68.6522	3.33632*E*-03
9	67.2152	4.26963*E*-03	9	61.7604	3.60853*E*-03
10	60.3375	4.69738*E*-03	10	55.4547	3.91964*E*-03
11	54.1154	5.55291*E*-03	11	49.8325	4.30852*E*-03
12	48.5908	6.09735*E*-03	12	44.7404	4.65850*E*-03
13	43.6592	7.22509*E*-03	13	40.1645	5.12514*E*-03
14	39.2786	8.43062*E*-03	14	35.7281	5.74735*E*-03
15	35.2050	9.98616*E*-03	15	32.1009	6.56400*E*-03
16	31.6405	0.0123194	16	28.8504	7.30288*E*-03
17	28.4318	0.0149249	17	25.9137	8.23620*E*-03
18	25.5091	0.0192804	18	23.2700	9.67504*E*-03
19	22.9143	0.0245692	19	20.8565	0.0114250
20	20.6054	0.0324245	20	18.7360	0.0137972
21	18.5058	0.0437021	21	16.8387	0.0168304
22	16.6503	0.0592573	22	15.0879	0.0216526
23	14.9832	0.0796346	23	13.5463	0.0277191
24	13.4765	0.106704	24	12.1721	0.0365856
25	12.1163	0.141000	25	10.9444	0.0487186
26	10.8886	0.181366	26	9.84931	0.0652071
27	9.76560	0.229003	27	8.85879	0.0867511
28	8.78904	0.279675	28	7.97291	0.113934
29	7.90316	0.330346	29	7.16376	0.148933
30	7.10796	0.377283	30	6.44530	0.189182
31	6.39647	0.418194	31	5.78961	0.235420
32	5.74775	0.455915	32	5.21064	0.283836
33	5.16879	0.485003	33	4.68749	0.327857
34	4.64564	0.507986	34	4.19921	0.373628
35	4.17828	0.526458	35	3.77371	0.416055
36	3.75976	0.540691	36	3.37611	0.448371
37	3.36913	0.551657	37	3.02734	0.477537
38	3.02734	0.561224	38	2.72042	0.500636
39	2.71344	0.567407	39	2.44140	0.517436
40	2.44140	0.573590	40	2.19726	0.529958
41	2.19726	0.577634	41	1.96707	0.540691
42	1.96010	0.581173	42	1.76478	0.549168
43	1.75781	0.584362	43	1.58342	0.555585
44	1.57645	0.586423	44	1.42299	0.561418
45	1.41601	0.588757	45	1.27650	0.565579
46	1.26953	0.590273	46	1.14397	0.569001
47	1.13699	0.591595	47	1.02539	0.571529
48	1.00446	0.593345	48	0.920757	0.573823
49	0.89983	0.594395	49	0.823101	0.576196
50	0.80915	0.595056	50	0.732420	0.577634

(continued)

Table 1 (continued)

PHOS			BISTRIS		
No.	p_{O_2}	Abs	No.	p_{O_2}	Abs
51	0.725445	0.596223	51	0.648715	0.579268
52	0.648715	0.596612	52	0.571985	0.580201
53	0.578961	0.597390	53	0.509206	0.581446
54	0.516182	0.598245	54	0.453403	0.582768
55	0.460378	0.598517	55	0.404575	0.583351
56	0.411550	0.599295			
57	0.369698	0.599451			

range of oxygen pressure data acquisition was expanded by using 2 channels of which one served the range from the maximum pressure down to 10% thereof, the other covering the range from 10% maximum pressure down to zero. The sampling of data points on the deoxygenation curve was carried out in such a way that each successive point was taken when its oxygen pressure value decreased to α times the last sampled value, where α was a selectable factor smaller than unity, typically being 0.9. The sampling of data points on the reoxygenation curve was made in the same way except that the factor was replaced by $1/\alpha$. Through this method of sampling, the data points were collected at constant intervals on a log p scale.

2.4. Analysis of oxygen equilibrium data

The analysis of equilibrium data was carried out with the computer described above. Programs were written in BASIC, compiled, and run on the operating system, MS-DOS (Microsoft Corp.).

The absorbance values were converted to oxygen saturation values using the equation,

$$Y_j = \frac{\mathrm{Abs}_j - \mathrm{Abs}_{\emptyset}}{\mathrm{Abs}_{\infty} - \mathrm{Abs}_{\emptyset}} = \frac{\mathrm{Abs}_j - \mathrm{Abs}_{\emptyset}}{\Delta \mathrm{Abs}_{\mathrm{T}}} \quad (j = 1\text{–}N), \tag{9}$$

where $\mathrm{Abs}_{\emptyset}$, Abs_{∞}, and Abs_j represent the values of the absorbance at $p = 0$, $p = \infty$, and p for the j-th point (p_j), respectively, $\Delta \mathrm{Abs}_{\mathrm{T}}$ the total absorbance change upon full oxygenation or reoxygenation, and N was the number of data points collected. $\mathrm{Abs}_{\emptyset}$ was determined by extrapolating the bottom portion of the curve toward $p = 0$ along an Abs_j vs p_j plot displayed on the CRT monitor of the computer. Abs_{∞} was determined either by graphical extrapolation of the top portion toward $p = \infty$ along an Abs_j vs $1/p_j$ plot [3,8,27] or by least-squares fitting together with As. In the graphical extrapolation, the quadratic function,

$$\mathrm{Abs} = ax^2 + bx + c \tag{10}$$

($x = p$ and $1/p$ for bottom and top extrapolations, respectively), was least-squares fitted to the endmost 15–18 data points in the bottom or top region and the best-fit c value was made equal to $\mathrm{Abs}_{\emptyset}$ or Abs_{∞}, respectively.

The Adair constants were evaluated by fitting eq. 1 to oxygen equilibrium curves by a least-squares method as previously described [3,8,28]. When $\mathrm{Abs}_{\emptyset}$ and Abs_{∞} were predetermined by extrapolation, the fitting was made on the (p_j, Y_j) data set. When Abs_{∞} was treated as an unknown parameter, the fitting was made on the (p_j,Abs_j) data set. These curve-fitting procedures were performed either with weighting or without weighting. The weight function used was

$$w_j^2 = N\left[Y_j(1 - Y_j)\right]^{-2} / \sum_{j=1}^{N} \left[Y_j(1 - Y_j)\right]^{-2} \tag{11}$$

which is based on an experimentally determined parabolic dependence of the standard error of Y (S_Y) on Y [9], i.e.,

$$S_Y = 0.08Y(1 - Y). \tag{12}$$

The asymmetric nature of the equilibrium curve was expressed by means of the symmetry index

(W) [29] defined by

$$W = \frac{K_1 K_4}{K_2 K_3} = \frac{A_1^2 A_4}{A_3^2}. \quad (13)$$

The curve is symmetric about the half-saturation point on the Hill plot when $W = 1$, while it becomes more asymmetric as the value of W becomes either smaller or larger than unity.

3. Results

Oxygen equilibrium curves were determined for purified Hb A at a concentration of 1.2 mM (on a heme basis) at 25 °C and pH 7.40 using either 0.1 M potassium phosphate buffer or 0.1 M Bis-Tris buffer containing 0.1 M Cl^-. The data obtained using phosphate and Bis-Tris are henceforth designated as 'PHOS data' and 'BISTRIS data', respectively. The raw data for deoxygenation curves are presented in table 1. The metHb contents in total Hb determined before and after oxygen equilibrium measurement are listed in table 2 together with the absorbance values at three wavelengths.

3.1. Least-squares fitting with weighting and Abs_∞ fixed

Fig. 1 shows the quadratic extrapolation of the bottom and top ends of the deoxygenation curve (PHOS data). The $Abs_\emptyset$ and Abs_∞ values thus

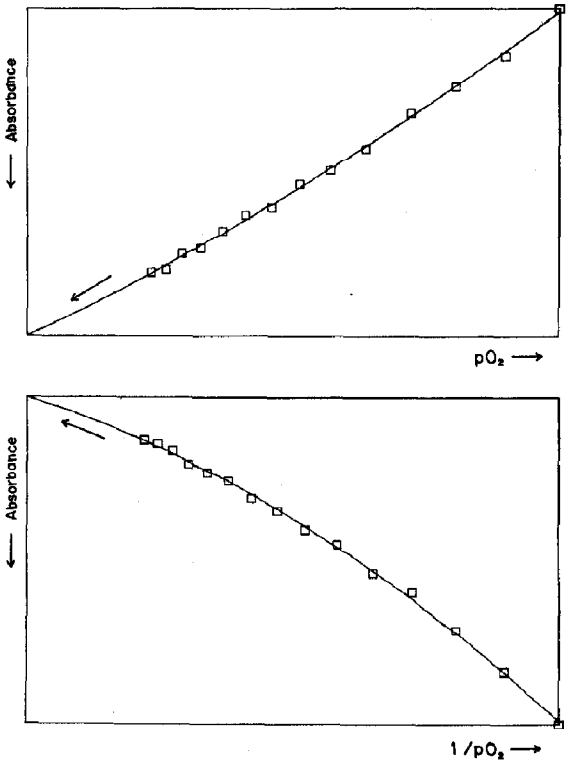

Fig. 1. Quadratic extrapolation of bottom end (upper) and top end (lower) of PHOS data (deoxygenation). Square symbols indicate observed points. Lines were calculated from eq. 10 and their end points on the ordinate gave $Abs_\emptyset = 0.60261$ and $Abs_\infty = 0.00044$ ($\Delta Abs_T = 0.60217$).

Table 2

Absorbance values and metHb content of hemoglobin samples [a]

	Absorbance at [b]			MetHb (%)
	560 nm	576 nm	630 nm	
PHOS data				
Before measurement	0.490	0.880	0.010	0.6
After measurement	0.481	0.850	0.014	2.3
BISTRIS data				
Before measurement	0.486	0.862	0.010	0.3
After measurement	0.472	0.835	0.013	1.9

[a] Immediately before and after oxygen equilibrium measurement, part of the sample was 22-fold diluted with 0.1 M phosphate buffer (pH 7.0) and its absorption spectrum was recorded.

[b] Light path length, 10 mm.

obtained are given in table 3 for PHOS data and in table 4 for BISTRIS data. The best-fit A values were obtained by the weighted least-squares method with $Abs_\emptyset$ and Abs_∞ fixed, and the results are listed in table 5. No negative A values occurred for this manner of analysis on the present equilibrium data. Table 5 also includes values of the stepwise Adair constants, K_i, oxygen pressure at half saturation, $P_{5\emptyset}$, median oxygen pressure [2,28], P_m, maximal slope of the Hill plot, n_{max}, and symmetry index, W, which were calculated from the A values. Both the deoxygenation and reoxygenation curves are presented as Hill plots in fig. 2, where the experimental plots are superimposed on lines calculated from the best-fit A values. Comparison of the parameter values in table 5 and of the plots in fig. 2 indicates that

Table 3

Parameter values obtained by least-squares curve fitting (PHOS data [a])

	A_1 ($mmHg^{-1}$)	A_2 ($mmHg^{-2}$)	A_3 ($mmHg^{-3}$)	A_4 ($mmHg^{-4}$)	Abs_∞	W
Weighted						
(A) Quadratic extrapolation	6.04×10^{-2}	1.38×10^{-3}	3.19×10^{-4}	2.55×10^{-4}	0.00044	9.14
(B) Abs_∞ increased by 0.1% of ΔAbs_T	5.60×10^{-2}	3.66×10^{-3}	1.57×10^{-4}	2.59×10^{-4}	0.00104	3.30×10
(C) Abs_∞ decreased by 0.1% of ΔAbs_T	6.30×10^{-2}	-6.58×10^{-5}	4.46×10^{-4}	2.52×10^{-4}	−0.00016	5.03
(D) Fitting with Abs_∞ floated	6.08×10^{-2}	1.36×10^{-3}	3.18×10^{-4}	2.56×10^{-4}	0.00046	9.36
(E) Fitting with $A_3 = 0$ and Abs_∞ floated	5.05×10^{-2}	6.24×10^{-3}	0 (fixed)	2.60×10^{-4}	0.00146	∞
Unweighted						
(F) Quadratic extrapolation	6.83×10^{-2}	1.92×10^{-3}	1.62×10^{-4}	2.53×10^{-4}	0.00044	4.50×10
(G) Abs_∞ increased by 0.1% of ΔAbs_T	6.66×10^{-2}	2.44×10^{-3}	9.77×10^{-5}	2.56×10^{-4}	0.00104	1.19×10^{2}
(H) Abs_∞ decreased by 0.1% of ΔAbs_T	6.99×10^{-2}	1.39×10^{-3}	2.26×10^{-4}	2.50×10^{-4}	−0.00016	2.39×10
(I) Fitting with Abs_∞ floated	5.96×10^{-2}	4.77×10^{-3}	-1.84×10^{-4}	2.69×10^{-4}	0.00362	2.82×10
(J) Fitting with $A_3 = 0$ and Abs_∞ floated	6.52×10^{-2}	3.11×10^{-3}	0 (fixed)	2.62×10^{-4}	0.00232	∞

[a] The results for the deoxygenation data are presented. The reoxygenation data gave similar results. Abs_0 was fixed at 0.60261 in all cases. Abs_∞ was fixed in cases A–C, F–H.

Table 4

Parameter values obtained by least-squares curve fitting (BISTRIS data [a])

	A_1 ($mmHg^{-1}$)	A_2 ($mmHg^{-2}$)	A_3 ($mmHg^{-3}$)	A_4 ($mmHg^{-4}$)	Abs_∞	W
Weighted						
(A) Quadratic extrapolation	7.52×10^{-2}	6.38×10^{-3}	1.73×10^{-3}	1.85×10^{-3}	0.00082	3.50
(B) Abs_∞ increased by 0.1% of ΔAbs_T	6.10×10^{-2}	1.61×10^{-2}	7.46×10^{-4}	1.88×10^{-3}	0.00140	1.26×10
(C) Abs_∞ decreased by 0.1% of ΔAbs_T	8.17×10^{-2}	1.34×10^{-3}	2.38×10^{-3}	1.82×10^{-3}	0.00023	2.14
(D) Fitting with Abs_∞ floated	7.76×10^{-2}	6.77×10^{-3}	1.60×10^{-3}	1.85×10^{-3}	0.00093	4.35
(E) Fitting with $A_3 = 0$ and Abs_∞ floated	4.42×10^{-2}	2.66×10^{-2}	0 (fixed)	1.89×10^{-3}	0.00166	∞
Unweighted						
(F) Quadratic extrapolation	8.77×10^{-2}	1.18×10^{-2}	4.98×10^{-4}	1.82×10^{-3}	0.00082	5.64×10
(G) Abs_∞ increased by 0.1% of ΔAbs_T	8.44×10^{-2}	1.34×10^{-2}	1.91×10^{-4}	1.84×10^{-3}	0.00140	3.60×10^{2}
(H) Abs_∞ decreased by 0.1% of ΔAbs_T	9.09×10^{-2}	1.02×10^{-2}	8.02×10^{-4}	1.80×10^{-3}	0.00023	2.31×10
(I) Fitting with Abs_∞ floated	7.09×10^{-2}	2.04×10^{-2}	-1.16×10^{-3}	1.94×10^{-3}	0.00395	7.25
(J) Fitting with $A_3 = 0$ and Abs_∞ floated	8.58×10^{-2}	1.37×10^{-2}	0 (fixed)	1.87×10^{-3}	0.00239	∞

[a] The results for the deoxygenation data are presented. The reoxygenation data gave similar results. Abs_0 was fixed at 0.58717 in all cases. Abs_∞ was fixed in cases A–C, F–H.

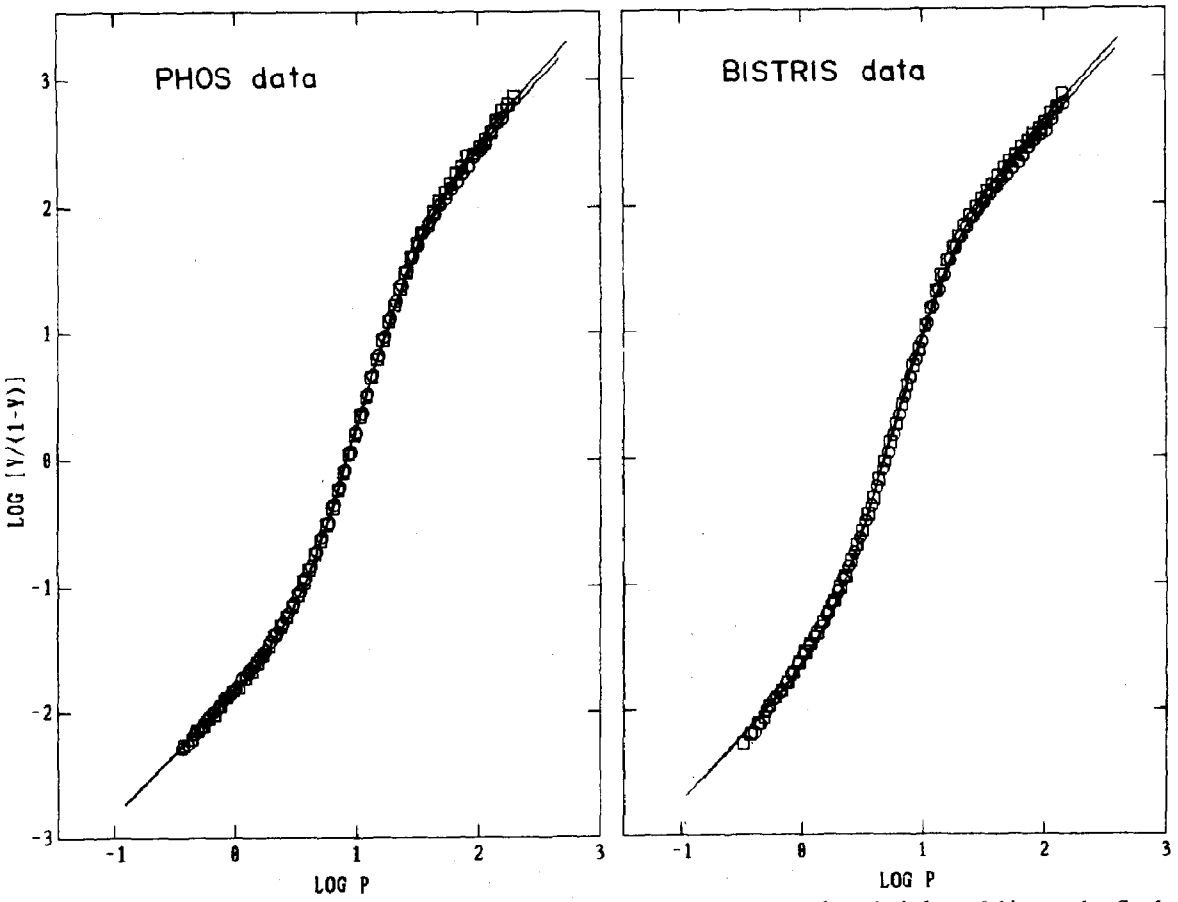

Fig. 2. Hill plots of deoxygenation (○) and succeeding reoxygenation (□) curves measured on single hemoglobin samples. Symbols indicate observed points and lines were calculated from the A values obtained by weighted least-squares analysis (case A in tables 3 and 4).

agreement between the deoxygenation and reoxygenation curves is excellent for both PHOS and BISTRIS data sets.

Because of this excellent agreement, only deoxygenation data will be presented in the ensuing text. However, identical results were also obtained for reoxygenation data in the succeeding analysis.

Since the asymptotic nature of the top end of the equilibrium curve is highly sensitive to the Abs_∞ value used, the extent to which the A values are influenced by minute changes in Abs_∞ value was also investigated. Fig. 3 shows top end extrapolations of PHOS deoxy data in which the Abs_∞ value at the ordinate intercept (i.e., the c value in eq. 10) was forced to increase or decrease by 0.1% of the ΔAbs_T value compared to the normally extrapolated value (fig. 1, lower). The extrapolated lines apparently deviate from the data points and look unnatural. The best-fit A values obtained with the altered Abs_∞ values are given in tables 3 and 4 (cf. cases B and C with case A). Upon minute changes in Abs_∞, the A_1 and A_4 values vary only slightly whereas those of A_2 and A_3 show marked variations in the opposite direction, the A_2 value for PHOS data even being negative. Fig. 4 shows how strongly the top portion of the Hill plot above 99% oxygen saturation ($\log[Y/(1-Y)] > 2$) is influenced by a change in Abs_∞ of only 0.1% of the ΔAbs_T value. Similar results were also reported previously [20,30].

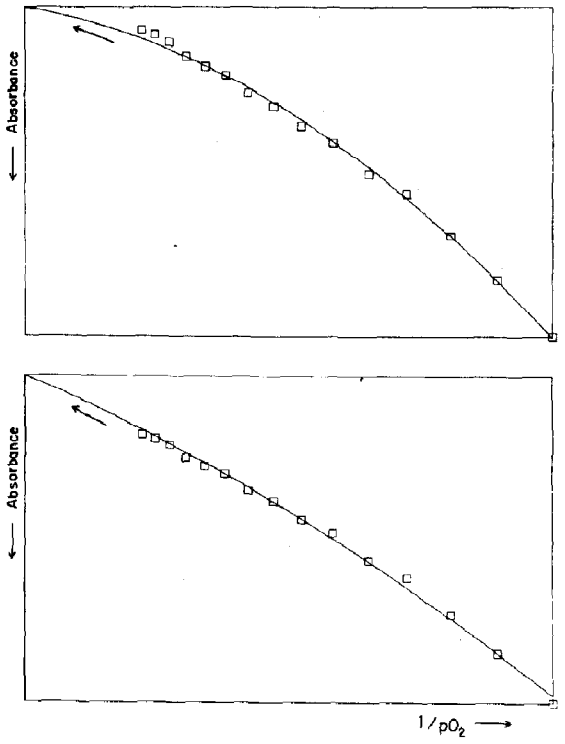

Fig. 3. Extrapolation of top end of PHOS data (deoxygenation). (Upper) Abs_∞ was increased by 0.1% of ΔAbs_T (in eq. 10, *a* and *b* were floated while *c* was fixed at 0.00044 + 0.00060 = 0.00104); (lower) Abs_∞ was decreased by 0.1% of ΔAbs_T ($c = -0.00016$).

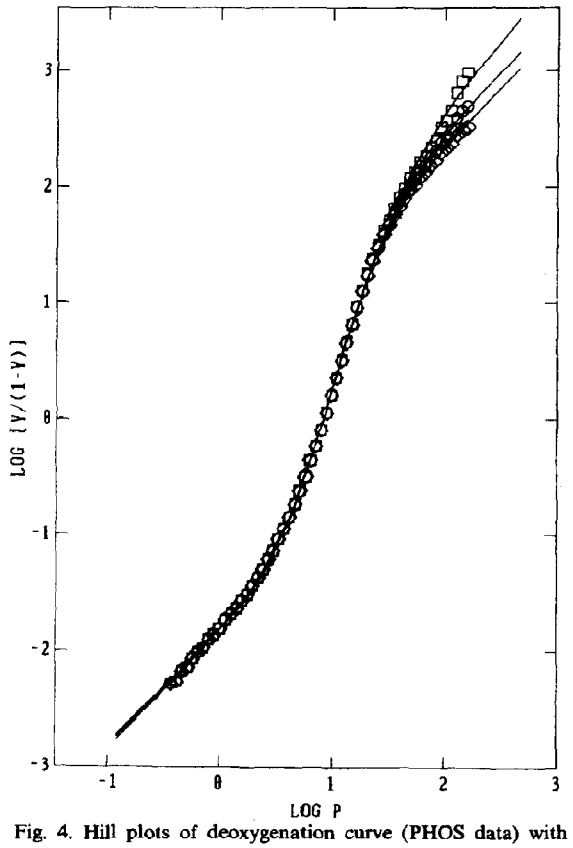

Fig. 4. Hill plots of deoxygenation curve (PHOS data) with different top end extrapolations. (○) Normal quadratic extrapolation (case A in table 3); (□) Abs_∞ was increased by 0.1% of ΔAbs_T (case B); (◇) Abs_∞ was decreased by 0.1% of ΔAbs_T (case C). Lines were calculated from the best-fit A values.

Table 5

Best-fit parameter values for deoxygenation and reoxygenation curves measured on single hemoglobin samples [a]

	PHOS		BISTRIS	
	Deoxy	Reoxy	Deoxy	Reoxy
A_1 ($mmHg^{-1}$)	6.04×10^{-2}	5.84×10^{-2}	7.52×10^{-2}	7.36×10^{-2}
A_2 ($mmHg^{-2}$)	1.38×10^{-3}	1.59×10^{-3}	6.38×10^{-3}	5.51×10^{-3}
A_3 ($mmHg^{-3}$)	3.19×10^{-4}	2.89×10^{-4}	1.73×10^{-3}	1.60×10^{-3}
A_4 ($mmHg^{-4}$)	2.55×10^{-4}	2.67×10^{-4}	1.85×10^{-3}	1.97×10^{-3}
K_1 ($mmHg^{-1}$)	1.51×10^{-2}	1.46×10^{-2}	1.88×10^{-2}	1.84×10^{-2}
K_2 ($mmHg^{-1}$)	1.52×10^{-2}	1.82×10^{-2}	5.66×10^{-2}	4.99×10^{-2}
K_3 ($mmHg^{-1}$)	3.47×10^{-1}	2.72×10^{-1}	4.07×10^{-1}	4.35×10^{-1}
K_4 ($mmHg^{-1}$)	3.20	3.69	4.28	4.93
P_{50} (mmHg)	8.22	8.13	4.92	4.84
P_m (mmHg)	7.91	7.82	4.82	4.75
n_{max}	3.21	3.23	3.18	3.23
W	9.14	1.09×10	3.50	4.17

[a] The bottom and top absorbance values were obtained by quadratic extrapolation. Best-fit A values were obtained by weighted least-squares analysis. Other parameters were calculated from the A values.

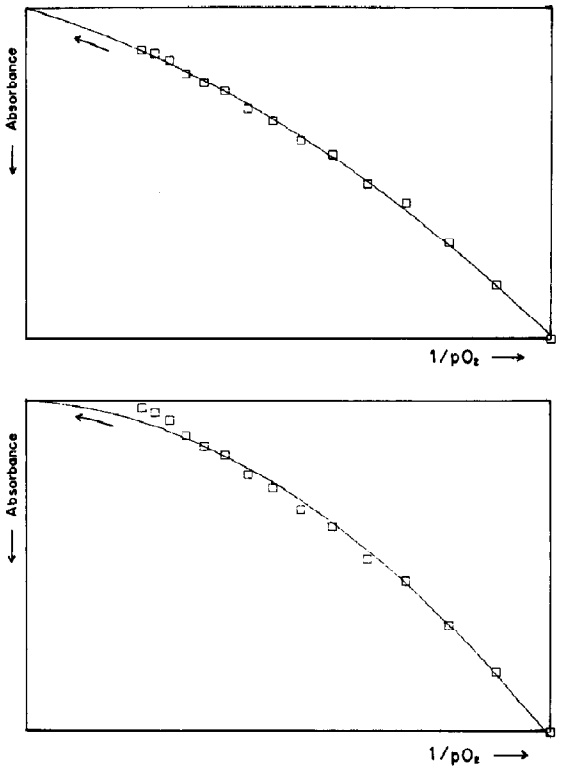

Fig. 5. Extrapolation of top end of PHOS data (deoxygenation). (Upper) With A_3 floated (case D in table 3); (lower) with A_3 fixed at 0 (case E). In both cases, Abs_∞ as well as the Adair constants was treated as an unknown parameter in the weighted least-squares analysis.

3.2. *Least-squares fitting with weighting and Abs_∞ floated*

It may be pointed out that the quadratic graphic extrapolation could introduce some subjective effect into the Abs_∞ value, since the goodness of fit in the extrapolation plot was judged by eye. Therefore, eq. 1 combined with eq. 9 was least-squares fitted to (p_j,Abs_j) data sets with $Abs_\emptyset$ fixed and Abs_∞ floated, and five parameters (four As and Abs_∞) were simultaneously evaluated. The top end extrapolation using the best-fit Abs_∞ value for PHOS data is shown in fig. 5 (upper). The best-fit parameter values are given in tables 3 and 4 (case D). They are virtually identical with those obtained through quadratic extrapolation by eye (case A), indicating that the possible subjective effect mentioned above is not a matter for concern.

Further least-squares fitting was performed with Abs_∞ floated and A_3 fixed at zero. In this case, the best-fit Abs_∞ value produces an unnatural extrapolation of the top end (see fig. 5, lower part). By forcing A_3 to be zero, the agreement between the experimental and calculated Hill plots becomes worse; the top portion of the experimental Hill plot wanders around the calculated line which has an asymptotic slope of 2 (fig. 6). Due to a compensating effect, the A_2 value is markedly increased when A_3 is forced to be zero (cf. case E with case D in tables 3 and 4).

3.3. *Least-squares fitting without weighting*

The present oxygen equilibrium data were analyzed through the same least-squares fitting

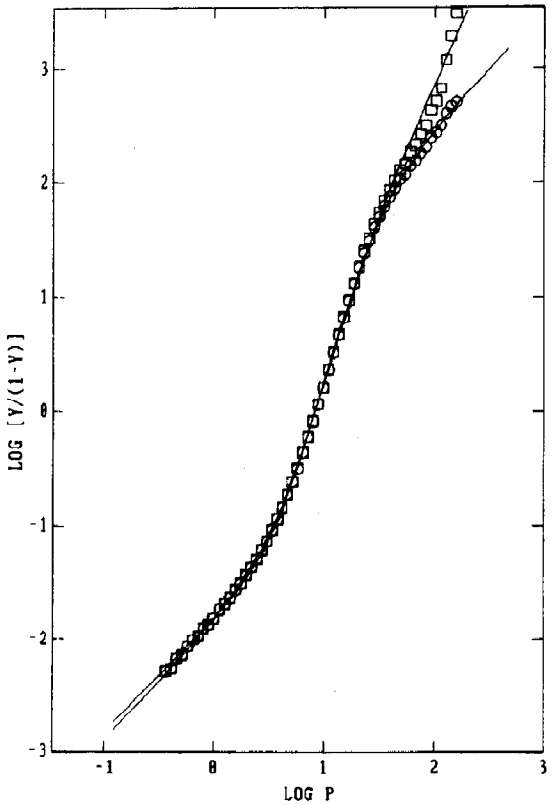

Fig. 6. Hill plots of deoxygenation curve (PHOS data). (○) With A_3 floated (case D in table 3); (□) with A_3 fixed at 0 (case E). Lines were calculated from the best-fit A values.

procedures as those labeled cases A–E in tables 3 and 4 except for using no weights, i.e., using equal weights. Cases F–J correspond to cases A–E, respectively.

When predetermined values of $Abs_{\emptyset}$ and Abs_{∞} were used (cases F–H), exactly the same phenomenon regarding the behavior of As as that noted in cases A–C was equally observed but the best-fit values of A_1, A_2, and A_3 were somewhat different from those obtained in weighted fitting. Interestingly, when Abs_{∞} was floated (case I), the A_3 value became negative for both PHOS and BISTRIS data. When A_3 was fixed at zero (case J), deviation between the experimental points and the calculated line at the top portion of the Hill plot was evident (fig. 7).

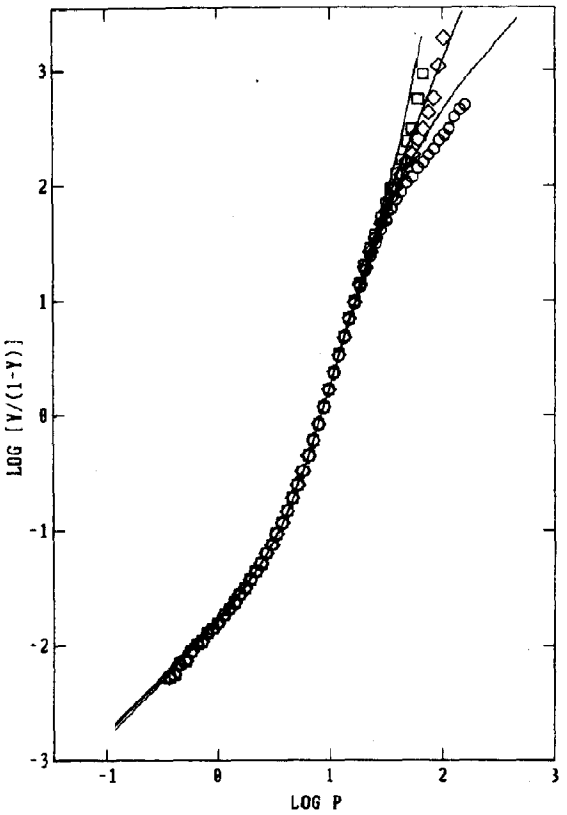

Fig. 7. Hill plots of deoxygenation curve (PHOS data) obtained by unweighted fitting. (○) With Abs_{∞} obtained by quadratic extrapolation (case F in table 3); (□) with Abs_{∞} floated (case I); (◇) with $A_3 = 0$ and Abs_{∞} floated (case J). Lines were calculated from the best-fit A values.

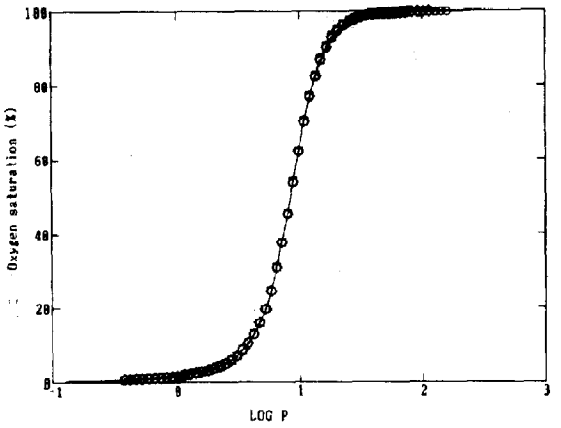

Fig. 8. Y vs log p plots of deoxygenation curve (PHOS data) obtained by unweighted fitting. Other details as in fig. 7.

As shown for cases F and I in fig. 7, the unweighted least-squares fitting shows a general trend that both the bottom and top portions of the calculated Hill lines deviate upward from the corresponding experimental plots. This indicates that the fitted curves are more asymmetric than those observed, as shown by increased values of W (tables 3 and 4).

Fig. 8 shows oxygen saturation vs log p plots of the same data as those plotted in fig. 7. Using this form of data presentation, resolution of the deviations between the top ends (also the bottom ends) of equilibrium curves is difficult, whereas it is readily achieved on the Hill plot where the end portions are enlarged.

4. Discussion

4.1. Problems and strategies: experimental aspects

To obtain true values of the Adair constants from the oxygen equlibrium curve, the hemoglobin sample must be of high purity with respect to contamination by minor hemoglobin components and derivatives other than the oxy or deoxy form, such as metHb and COHb, and dissociated forms. The present experiments using purified, concentrated Hb A samples with low levels of metHb satisfy these conditions.

To determine a highly accurate oxygen equilibrium curve both the hemoglobin sample and the apparatus must be stable enough during measurement. The degree of stability is judged from the agreement between the deoxygenation and reoxygenation curves measured for a single hemoglobin sample. The reversibility of oxygenation, i.e., the agreement between the two curves, is an important criterion that allows us to feel confident of having observed the 'equilibrium' [3,10]. Any changes other than those of the absorbance associated with oxygenation and reoxygenation can be factors affecting the reversibility; namely, metHb formation, protein denaturation, aggregation or dissociation, drift of apparatus, etc. In the present study the increment in metHb content during measurement was only 1.6–1.7% (table 2). The maximum drift of zero baseline for the spectrophotometer used is 0.0004 absorbance units per h as described in the instruction manual and confirmed by the author. This drift amounts to only 0.067% of the typical ΔAbs_T value (0.6), and this percent value is smaller than the ΔAbs_T change (0.1%) intentionally introduced into the extrapolation tests for the top end of the plots (see section 3). The excellent agreement between the deoxygenation and reoxygenation curves as demonstrated on the Hill plots (fig. 2) and by the best-fit parameter values (table 5) proves that true equilibrium curves were indeed determined in the present study.

The importance of reversibility has been recognized by few investigators. Gill et al. [13] presented one data set which showed agreement between deoxygenation and reoxygenation curves (see data set $J + J^*$ in their paper). However, their reversibility test was not sufficiently strict, since reoxygenation was achieved only up to $p =$ 30 mmHg ($Y = 0.986$) while deoxygenation started at $p = 450$ mmHg ($Y = 0.999$). Further, their data set showed a significant difference in ΔAbs_T between the deoxygenation (0.1269) and reoxygenation (0.0971) curves, indicating that some irreversible change contributing to 23% of ΔAbs_T occurred during measurement. Compared to their thin-layer cell, our apparatus has the advantage that the top portion of the equilibrium curve to which A_3 is sensitive can be measured rapidly in both forward and reverse directions, since only a small amount of oxygen combines or dissociates in this region. This minimizes the effect of sample and machine instability and provides accurate data suitable for exploring the asymptotic properties of the top portion.

The reliability of the best-fit parameter values becomes greater as the number of data points per equilibrium curve increases [31]. With our apparatus this number can easily be increased by using a sampling factor, α, closer to unity with no change in total measurement time. On the other hand, with Gill's thin-layer cell, the measurement time becomes longer in proportion to the number of data points, since complete establishment of equilibrium is required upon every stepwise change in p. The measurement time cannot be prolonged very much due to the limited stability of hemoglobin samples. Decrease in the thickness of the layer reduces the equilibration time, but ΔAbs_T becomes smaller, thus impairing the spectrophotometric accuracy. In fact, the small ΔAbs_T value (approx. 0.1) of Gill's group as compared to ours (approx. 0.6) can cause loss in resolution due to lowered signal-to-noise ratio [31].

4.2. Problems and strategies: analytical aspects

The author has stressed the importance of correct extrapolation of both ends of the oxygen equilibrium curve [3,10,27]. To make unequivocal extrapolations possible, the equilibrium data must be collected over a wide range of saturation. The Hill plot is very useful for a diagnostic test of equilibrium data. To resolve the asymptotic nature of the Hill plot for Hb A under the usual experimental conditions, it is necessary to measure oxygen saturation from 1 to 99.9% [3,8]. Because of the asymmetric nature of the equilibrium curve, extrapolation of the bottom part is easier than that of the top. Therefore, Abs_0 was fixed at a constant value while Abs_∞ was changed or floated in the present analysis.

The present analysis shows that even a 0.1% change in Abs_∞ can cause significant changes in the shape of the upper portion of the Hill plot (fig. 4) and in the best-fit Adair constants (tables 3 and 4). Based on a similar analysis, Marden et al. [20]

concluded that unique solutions for the R-state affinity and populations of intermediate states may be impossible to achieve, since the differences in that affinity and fraction of the triply liganded species are within the experimental errors of a few parts per thousand. However, the present study indicates that careful determination of the upper extreme enables one to resolve even a 0.1% change of Abs_∞ on the Abs vs $1/p$ plot (fig. 3) and such efforts are hence worthwhile in order to achieve unique solutions.

Gill's group [13] employed equal weighting in their least-squares fitting procedure. This manner of weighting (i.e., unweighting) can be appropriate when the residuals are evenly distributed throughout the equilibrium curve. However, the actual distributions are apparently uneven (see fig. 2 of ref. 13), suggesting that heavier weights should be applied to both ends.

We used a parabolic weight function (eq. 11) which is based on eq. 12. As previously pointed out, the curve fitting using this weighting is equivalent to that using equal weighting on the Hill plot [3,8]. The explanation for obtaining the error distribution of Y (eq. 12) in spite of even error in absorbance measurement is as follows. In our least-squares analysis, the independent variable (p) is treated as error-free and its error is incorporated into the dependent variable (Y). The relative error, $\delta p/p$, rather than δp itself, and therefore the error of log p, is nearly constant in the major, intermediate region of saturation [9]. This results in a parabolic distribution of error for Y, since a minute shift of the Y vs log p plot along the abscissa produces a change of Y which shows a bell-shaped dependence on Y.

The present analysis showed that the choice of weighting has a quite different consequence. On fitting with equal weighting and Abs_∞ floated, negative A_3 values were obtained whereas, on fitting with weighting, the A_3 value was always positive irrespective of whether Abs_∞ was fixed or floated (tables 3 and 4). The former way of fitting probably reproduces the situation encountered by Gill's group. It was pointed out that equally weighted fitting results in an unusually small value for A_3 [31].

4.3. Magnitude of A_3 value

The author concludes that (a) the major cause for the occurrence of a zero (or negative) A_3 value in the analysis of Gill et al. is the use of equal weighting and (b) the zero A_3 value cannot be accommodated within accurate equilibrium data.

In the analysis of Gill et al., a small 'negative' fitted value for A_3 was obtained in virtually all cases when constraints on the A terms to be positive were removed [13]. This means that their raw data or adequacy of their analysis, or both, should be reexamined; otherwise they should have obtained physically meaningful positive values, or, at least, values randomly distributed around zero for A_3.

The present equilibrium data are not consistent with an asymptotic slope of 2 for the upper end of the Hill plot and, consequently, with a zero A_3 value. When A_3 is forced to be zero, the top end extrapolation and the top portion of the Hill plot show apparent disagreement between observed and fitted data (figs 5 and 6). Such disagreement also occurs when equal weighting is used (fig. 7). The present analysis with normal end extrapolation and weighting consistently gave positive A_3 values which are comparable to A_4 values (table 5). These values yield K_4 values ranging from 3 to 5 (refer to eq. 4). The zero A_3 value makes the K_R value as large as 21 $mmHg^{-1}$ [32] which is inconsistent with the generally accepted affinity for the R state [20].

4.4. Criteria for correct determination of the Adair constants

The following criteria are given. (a) Deoxygenation and reoxygenation curves must agree throughout the entire range of saturation. (b) The weighting used in least-squares fitting must be appropriate; it must be determined from experimental error distribution data. (c) Positive values for As must be obtained without any constraint on them. (d) There must be no systematic deviation between the experimental and fitted curves. (e) Agreement between given equilibrium curves must be tested on the Hill plot, not on the conventional

Y vs log p plot; it is impossible on the latter to resolve small deviations on the top portion which are distinct on the former (cf. fig. 8 with fig. 7).

Acknowledgements

The author thanks Mr. H. Minagawa for providing purified hemoglobin samples. This work was supported in part by Ajinomoto Co., Tokyo.

References

1 G.S. Adair, J. Biol. Chem. 63 (1925) 529.
2 J. Wyman, Adv. Protein Chem. 19 (1964) 223.
3 K. Imai, Allosteric effects in haemoglobin (Cambridge University Press, Cambridge, 1982).
4 F.J.W. Roughton, A.B. Otis and R.L.J. Lyster, Proc. Roy. Soc. Lond. B144 (1955) 29.
5 F.J.W. Roughton, Clin. Chem. 9 (1963) 682.
6 F.J.W. Roughton and R.L.J. Lyster, Hvalradets Skr. 48 (1965) 185.
7 K. Imai, J. Mol. Biol. 133 (1979) 233.
8 K. Imai, Methods Enzymol. 76 (1981) 470.
9 K. Imai, H. Morimoto, M. Kotani, H. Watari, W. Hirata and M. Kuroda, Biochim. Biophys. Acta 200 (1970) 189.
10 K. Imai, Methods Enzymol. 76 (1981) 438.
11 D. Dolman and S.J. Gill, Anal. Biochem. 87 (1978) 127.
12 S.J. Gill, Methods Enzymol. 76 (1981) 427.
13 S.J. Gill, E. Di Cera, M.L. Doyle, G.A. Bishop and C.H. Robert, Biochemistry 26 (1987) 3995.
14 E. Di Cera, M.L. Doyle and S.J. Gill, J. Mol. Biol. 200 (1988) 593.
15 M.L. Doyle, E. Di Cera, C.H. Robert and S.J. Gill, J. Mol. Biol. 196 (1987) 927.
16 E. Di Cera, M.L. Doyle, P.R. Connelly and S.J. Gill, Biochemistry 26 (1987) 6494.
17 G.K. Ackers and H.R. Halvorson, Proc. Natl. Acad. Sci. U.S.A. 71 (1974) 4312.
18 G.K. Ackers, M.L. Johnson, F.C. Mills, H.R. Halvorson and S. Shapiro, Biochemistry 14 (1975) 5128.
19 M.L. Johnson and G.K. Ackers, Biophys. Chem. 7 (1977) 77.
20 M.C. Marden, J. Kister, C. Poyart and S.J. Edelstein, J. Mol. Biol. 208 (1989) 341.
21 C. Nozaki and C. Tanford, Methods Enzymol. 11 (1967) 733.
22 K. Imai, Y. Yoshioka, I. Tyuma and M. Hirano, Biochim. Biophys. Acta 668 (1981) 1.
23 O.W. van Assendelft and W.G. Zijlstra, Anal. Biochem. 69 (1975) 43.
24 K. Imai and T. Yonetani, Biochim. Biophys. Acta 490 (1977) 164.
25 R.E. Lynch, G.R. Lee and G.E. Cartwright, J. Biol. Chem. 251 (1976) 1015.
26 C.C. Winterbourn, B.M. McGrath and R.W. Carrell, Biochem. J. 155 (1976) 493.
27 K. Imai and T. Yonetani, J. Biol. Chem. 250 (1975) 2227.
28 K. Imai, Biochemistry 12 (1973) 798.
29 D.W. Allen, K.F. Guthe and J. Wyman, J. Biol. Chem. 187 (1950) 393.
30 K. Imai, Symposium on oxygen binding heme proteins, Pacific Grove, CA, 1988, LVI-4.
31 D. Myers, K. Imai and T. Yonetani, Biophys. Chem. 37 (1990) 323.
32 E. Di Cera, C.H. Robert and S.J. Gill, Biochemistry 26 (1987) 4003.